arXiv:physics/0410215v1 [physics.plasm-ph] 22 Oct 2004

Electron cyclotron current drive efficiency in an axisymmetric tokamak

C. Gutiérrez-Tapia and M. Beltrán-Plata

Departamento de Física, Instituto Nacional de Investigaciones Nucleares
A. Postal 18-1027, 11801 México D. F., MEXICO

E-mail: `cgt@nuclear.inin.mx`

Abstract. The neoclassical transport theory is applied to calculate electron cyclotron current drive (ECCD) efficiency in an axisymmetric tokamak in the low-collisionality regime. The tokamak ordering is used to obtain a system of equations that describe the dynamics of the plasma where the nonlinear ponderomotive (PM) force due to high-power RF waves is included. The PM force is produced around an electron cyclotron resonant surface at a specific poloidal location. The ECCD efficiency is analyzed in the cases of first and second harmonics (for different impinging angles of the RF waves) and it is validated using experimental parameter values from TCV and T-10 tokamaks. The results are in agreement with those obtained by means of Green's function techniques.

PACS numbers: 52.55.Wq, 52.35.Mw, 52.40.Db

1. Introduction

Electron cyclotron waves can efficiently drive a localized non-inductive current in toroidal devices for a number of applications. The main of these are found in the neoclassical tearing mode control [1], the fully non-inductive current drive in tokamaks [2, 3] and the bootstrap current compensation in stellerators [4]. ECCD results from the sensitive heating of electrons travelling in one direction in order to decrease their collision frequency, and thus enhance their contribution to the toroidal current, compared to their unheated counterparts moving in the opposite direction [5]. For an off-axis current drive, this current drive mechanism is offset by the mirror trapping of electrons in toroidal geometries that drives current in the reverse direction [6]. The ECCD efficiency is usually calculated through a bounce-averaged quasilinear Fokker-Planck treatment [7, 8].

Electron cyclotron (EC) waves have recently attracted a great interest. Such waves exhibit the very important property of being able to be excited at a localized particular magnetic surface. This mechanism considers the introduction of EC waves at a minimum of the magnetic field, where the resonance condition $\upsilon_{zr} = \left(\omega - \omega_{Be}\right)/k_z$ holds. Many tokamak experiments have reported that the ECCD efficiency decreases as the power deposition location is moved away from the plasma center, either by varying the magnetic field strength [9] or by changing the poloidal steering of the ECCD launcher [10].

In the low power limit, the ECCD can be calculated from the relativistic, linearized Fokker-Planck equation using ray tracing codes [11]. If the effects of the radiofrequency (RF) quasilinear diffusion and the parallel electric field are included, the bounce-averaged, quasilinear Fokker-Planck codes can be used [12]. However, the nonlinearities associated to high power effects are not considered. In the present paper we analyze the ECCD efficiency in an axisymmetric tokamak, in the low collisionallity regime within the neoclassical transport theory. The ECCD is calculated including a ponderomotive force $\mathcal{F}$. The tokamak ordering is used to obtain a system of equations that describe the dynamics of the plasma where the nonlinear ponderomotive (PM) force due to high-power RF waves is included. The PM force is produced around an electron cyclotron resonant surface at a specific poloidal location. The ECCD efficiency is analyzed in the cases of the first and second harmonics (for different impinging angles of the RF waves) and it is validated using experimental parameter values from TCV and T-10 tokamaks. The results obtained are in agreement with those delivered by the linearized Fokker-Planck equation.

2. Basic equations.

Let us assume a plasma which contains only charged and neutral particles in a toroidal axysimmetric magnetic field. The hydrodynamic description of the plasma is taken in the neoclassical fluid approximation. In this approach, the continuity equation for the averaging quantities respecting the RF field becomes

$$\frac{\partial n_\alpha}{\partial t} + \nabla \cdot (\eta_\alpha \mathbf{U}_\alpha) = S_{n\alpha}, \tag{1}$$

where $S_{n\alpha}$ is the source term obeying the condition

$$\sum_\alpha q_\alpha S_{n\alpha} = \sum_\alpha q_\alpha \int \left(\frac{\partial f_\alpha}{\partial t} \right)_{s0} d\mathbf{v} = 0. \tag{2}$$

where $S_{n\alpha} = \int \left(\partial f_\alpha / \partial t \right)_s d\mathbf{v}$. For the moment equation, we have

$$m_\alpha \frac{\partial \left(n_\alpha \mathbf{U}_\alpha \right)}{\partial t} = -\nabla \cdot \widehat{\mathbf{P}}_\alpha - m_\alpha \nabla \cdot \left(n_\alpha \mathbf{U}_\alpha \mathbf{U}_\alpha \right) + \mathbf{R}_{c0}^{(\alpha)} + \mathbf{R}_{s0}^{(\alpha)} \\ + q_\alpha \left[n_\alpha \mathbf{E}_0 + \frac{1}{c} n_\alpha \mathbf{U}_\alpha \times \mathbf{B}_0 \right] + \mathbf{F}_{v\alpha} - \nabla \cdot \widehat{\pi}_\alpha, \tag{3}$$

The subindex α refers to the particle species; m_α, n_α, and U_α are the mass, electric charge, the density of particles and the velocity of the fluid, respectively. F_α is the ponderomotive force, π_α is the viscosity tensor and, finally, p_α is the pressure defined by $p_\alpha = n_\alpha T_\alpha$, where T_α is the plasma temperature. On the other hand,

$$R_{c0}^{(\alpha)} = m_\alpha \int \left(\frac{\partial f_\alpha}{\partial t} \right)_{c0} dv; \tag{4}$$

$$R_{s0}^{(\alpha)} = m_\alpha \int \left(\frac{\partial f_\alpha}{\partial t} \right)_{s0} dv, \tag{5}$$

is the force of friction between the particles of species α with neutrals.

The system of equations (1) and (3) must be completed with the Maxwell equations for the averaging quantities

$$\begin{aligned} \nabla \cdot \mathbf{E} &= 4\pi q_\alpha n_{\alpha 0}, \\ \nabla \times \mathbf{E} &= -\frac{1}{c} \frac{\partial \mathbf{B}}{\partial t}, \\ \nabla \cdot \mathbf{B} &= 0, \\ \nabla \times \mathbf{B} &= \frac{1}{c} \frac{\partial \mathbf{E}}{\partial t} + \frac{4\pi}{c} q_\alpha n_{\alpha 0} \mathbf{U}_\alpha. \end{aligned} \tag{6}$$

By using an standard expansion with respect to the ratio of the gyroradius and the characteristic length, it follows that

$$\varepsilon = \frac{\rho_{L\alpha}}{L},$$

where $\rho_{L\alpha}$ is the Larmor radius and L is the characteristic length [13].

3. Equations of zeroth and firsth orders.

The system of equations (1)-(3) is reduced, to zero-th order terms, to

$$\nabla \cdot n_{\alpha 0} \mathbf{U}_{\alpha 0} = 0, \tag{7}$$

$$\nabla \cdot \widehat{\mathbf{P}}_\alpha = q_\alpha \left[n_{\alpha 0} \mathbf{E}_0 + \frac{1}{c} n_{\alpha 0} \mathbf{U}_{\alpha 0} \times \mathbf{B}_0 \right], \tag{8}$$

and the Maxwell equations become

$$\begin{aligned} \nabla\cdot\mathbf{E}_0 &= 0,\\ \nabla\times\mathbf{E}_0 &= 0,\\ \nabla\cdot\mathbf{B}_0 &= 0,\\ \nabla\times\mathbf{B}_0 &= \frac{4\pi}{c}\mathbf{J}_{\alpha 0}. \end{aligned} \tag{9}$$

Here, we obtain that $\mathbf{E}_0 = -\nabla\Phi_0$

In this case, the solution of the system (7)-(8) has the form

$$U_\alpha^\psi = 0, \tag{10}$$

$$U_\alpha^\theta = \frac{c}{B_0^2}\left[\frac{\partial\Phi_0}{\partial\psi} + \frac{1}{q_\alpha n_{\alpha 0}}\frac{\partial p_\alpha}{\partial\psi}\right]\frac{B_{0\theta}B_0^\theta}{JB_0^\zeta} + \lambda\left(\psi\right)B_0^\theta, \tag{11}$$

$$U_\alpha^\zeta = -\frac{c}{B_0^2}\left[\frac{\partial\Phi_0}{\partial\psi} + \frac{1}{q_\alpha n_{\alpha 0}}\frac{\partial p_\alpha}{\partial\psi}\right]\frac{B_{0\zeta}B_0^\zeta}{JB_0^\theta} + \lambda\left(\psi\right)B_0^\zeta. \tag{12}$$

where we have introduced the toroidal flux coordinates (ψ,θ,ζ). Within this coordinate system, the contravariant forms of the magnetic field and of the fluid velocity for an axisymmetric tokamak are written as

$$\begin{aligned} \mathbf{B}_0 &= I\left(\psi\right)\nabla\zeta + \nabla\zeta\times\nabla\psi,\\ \mathbf{U}_\alpha &= U_\alpha^\theta\mathbf{e}_\theta + U_\alpha^\zeta\mathbf{e}_\zeta, \end{aligned} \tag{13}$$

where $n_{\alpha 0} = cte$ and the function $\lambda\left(\psi\right)$ is unknown.

Considering the inequality $B_{0\zeta}B_0^\zeta \gg B_{0\theta}B_0^\theta$ and $B_0^2 \simeq B_{0\zeta}B_0^\zeta$ we reduce the equations (11) and (12) to the form

$$U_\alpha^\theta = \lambda\left(\psi\right)B_0^\theta; \tag{14}$$

$$U_\alpha^\zeta = -\frac{c}{JB_0^\theta}\left[\frac{\partial\Phi_0}{\partial\psi} + \frac{1}{q_\alpha n_{\alpha 0}}\frac{\partial p_\alpha}{\partial\psi}\right] + \lambda\left(\psi\right)B_0^\zeta. \tag{15}$$

which are the zero-th order velocity equations. The corresponding toroidal current density is calculated from the relationship

$$\begin{aligned} j^\zeta &\equiv q_\alpha n_\alpha U_\alpha^\zeta\\ &= -\frac{cq_\alpha n_\alpha}{JB_0^\theta}\left[\frac{\partial\Phi_0}{\partial\psi} + \frac{1}{q_\alpha n_{\alpha 0}}\frac{\partial p_\alpha}{\partial\psi}\right] + q_\alpha n_\alpha\lambda\left(\psi\right)B_0^\zeta. \end{aligned} \tag{16}$$

Equations (1)-(3) containing terms to first order. Ignoring the source term they become

$$\frac{\partial n_{\alpha 0}}{\partial t} + \nabla\cdot\left(n_{\alpha 0}\mathbf{U}_\alpha\right) = 0, \tag{17}$$

$$\begin{aligned} m_\alpha\frac{\partial\left(n_{\alpha 0}\mathbf{U}_\alpha\right)}{\partial t} &= -\nabla p_\alpha - \nabla\cdot\widehat{\pi}_\alpha - m_\alpha\nabla\cdot\left(n_{\alpha 0}\mathbf{U}_\alpha\mathbf{U}_\alpha\right) + \mathbf{R}_\alpha^{(\alpha.n)}\\ &+ q_\alpha\left[n_{\alpha 0}\mathbf{E}_0 + \frac{1}{c}n_{\alpha 0}\mathbf{U}_\alpha\times\mathbf{B}_0\right] + \mathcal{F}_\alpha, \end{aligned} \tag{18}$$

where $\widehat{\mathbf{P}}_\alpha = p_\alpha + \widehat{\pi}_\alpha$, p_α is the scalar pressure, $\widehat{\pi}_\alpha$ is the viscosity tensor, $\mathbf{R}_\alpha^{(\alpha.n)} = \mathbf{R}_{c0}^{(\alpha)} + \mathbf{R}_{s0}^{(\alpha)}$ is the friction force from the particles of species α with neutrals and $\mathcal{F}_\alpha = \mathbf{F}_{v\alpha} - \nabla\cdot\widehat{\pi}_\alpha$ is the average ponderomotive force associated with the RF field acting on the particles.

4. Steady state equations.

In a steady state, the above system of equations can be written in the form

$$\begin{aligned} \nabla\cdot\left(\eta_{\alpha 0}\mathbf{U}_\alpha\right) &= 0, \qquad (19)\\ m_\alpha\nabla\cdot\left(\eta_{\alpha 0}\mathbf{U}_\alpha\mathbf{U}_\alpha\right) &= -\nabla p_\alpha-\nabla\cdot\widehat{\pi}_\alpha+\mathbf{R}_\alpha^{(\alpha..n)}\\ &\quad+q_\alpha\left[n_{\alpha 0}\mathbf{E}_0+\frac{1}{c}n_{\alpha 0}\mathbf{U}_\alpha\times\mathbf{B}_0\right]+\mathcal{F}_\alpha, \qquad (20)\end{aligned}$$

where the ζ component of the velocity becomes

$$\begin{aligned} U_\alpha^\zeta = &-\frac{c}{B_0^2}\left(\frac{\partial\Phi_0}{\partial\psi}+\frac{1}{q_\alpha n_{\alpha 0}}\frac{\partial p_\alpha}{\partial\psi}\right)\frac{B_{0\zeta}B_0^\zeta}{JB_0^\theta}+\frac{B_0^\zeta}{\mu_0\cdot\mathbf{B}_0}\left\{\left\langle\mathbf{B}_0\cdot\mathcal{F}_\alpha\right\rangle-k\right.\\ &\left.-\frac{c}{B_0^2}\left(\frac{\partial\Phi_0}{\partial\psi}+\frac{1}{q_\alpha n_{\alpha 0}}\frac{\partial p_\alpha}{\partial\psi}\right)\left[\frac{\mu_\theta B_{0\theta}B_0^\theta}{JB_0^\zeta}-\frac{\mu_\zeta B_{0\zeta}B_0^\zeta}{JB_0^\theta}\right]\right\}, \qquad (21)\end{aligned}$$

where μ_θ and μ_ζ are the poloidal and toroidal coefficients of viscosity, respectively. In the limit $B_{0\theta}B_0^\theta << B_{0\zeta}B_0^\zeta$ and $B_0^2\approx B_{0\zeta}B_0^\zeta$, the toroidal current density is reduced to

$$\begin{aligned} j^{(\zeta)} = &-\frac{cn_\alpha q_\alpha}{JB_0^\theta}\left[\frac{\partial\Phi_0}{\partial\psi}+\frac{1}{q_\alpha n_{\alpha 0}}\frac{\partial p_\alpha}{\partial\psi}\right]+\frac{n_\alpha q_\alpha B_0^\zeta}{\left(\mu_0\cdot\mathbf{B}_0\right)+m_\alpha n_{\alpha 0}v_{\alpha n}\left\langle B_0^2\right\rangle}\left\{\left\langle\mathbf{B}_0\cdot\mathcal{F}_\alpha\right\rangle-k\right.\\ &\left.+\frac{c\mu_\zeta}{JB_0^\theta}\left[\frac{\partial\Phi_0}{\partial\psi}+\frac{1}{q_\alpha n_{\alpha 0}}\frac{\partial p_\alpha}{\partial\psi}\right]+m_\alpha n_{\alpha 0}v_{\alpha n}\frac{c\left\langle B_{0\zeta}\right\rangle}{JB_0^\theta}\left[\frac{\partial\Phi_0}{\partial\psi}+\frac{1}{q_\alpha n_{\alpha 0}}\frac{\partial p_\alpha}{\partial\psi}\right]\right\}, \qquad (22)\end{aligned}$$

and

$$\begin{aligned} \lambda\left(\psi\right) = &\frac{1}{\left(\mu_0\cdot\mathbf{B}_0\right)+m_\alpha\eta_{\alpha 0}v_{\alpha n}\left\langle B_0^2\right\rangle}\left\{\left\langle\mathbf{B}_0\cdot\mathcal{F}_\alpha\right\rangle-k+\frac{c\mu_\zeta}{JB_0^\theta}\left[\frac{\partial\Phi_0}{\partial\psi}+\frac{1}{q_\alpha\eta_{\alpha 0}}\frac{\partial p_\alpha}{\partial\psi}\right]\right.\\ &\left.+m_\alpha\eta_{\alpha 0}v_{\alpha n}\frac{c\left\langle B_{0\zeta}\right\rangle}{JB_0^\theta}\left[\frac{\partial\Phi_0}{\partial\psi}+\frac{1}{q_\alpha\eta_{\alpha 0}}\frac{\partial p_\alpha}{\partial\psi}\right]\right\}. \qquad (23)\end{aligned}$$

5. The ponderomotive force.

The RF ponderomotive force has several representations according to its functionality with respect to time. In this work, we chose the following expression of the time averaged ponderomotive force [14]

$$\mathcal{F}_\alpha=\frac{1}{2}Re\left\{\frac{i}{\omega}\nabla E^*\cdot\mathbf{j}_\alpha-\nabla\cdot\left[\mathbf{j}_\alpha\left(\frac{i}{\omega}E^*+\frac{4\pi\mathbf{j}_\alpha^*}{\omega_{p\alpha}^2}\right)\right]\right\}, \qquad (24)$$

where ω is the frequency of the RF wave, $\mathbf{j}_\alpha$ is the current density of particles of species α induced by the RF field $\mathbf{E}$ and $\omega_{p\alpha}^2=4\pi n_\alpha q_\alpha^2/m_\alpha$ is the plasma frequency of particles of species α.

Given the Ohm's law, we assume the conductivity tensor σ_{jk}, which depends on the assumed characteristic frequency. The ponderomotive force is introduced thanks to a system of orthogonal coordinates $(\mathbf{e}_1,\mathbf{e}_2,\mathbf{e}_3)$ with the components of the conductivity tensor in the form

$$\sigma_{11}=\sigma_{22}=\frac{i\omega}{4\pi}\frac{\upsilon}{1-u};\qquad \sigma_{12}=-\sigma_{21}=-\frac{\omega}{4\pi}\frac{\sqrt{u}\upsilon}{1-u}, \qquad (25)$$

Table 1. TCV tokamak data for the first and second harmonics.

	B_0 (gauss)	n_e (cm^{-3})	a (cm)	R_0 (cm)	P (MW)	T_e (KeV)	q
1th harmonic	1.43×10^4	1.75×10^{13}	25.0	88.0	1.0	3.5	10
2nd harmonic	1.43×10^4	1.75×10^{13}	25.0	88.0	1.0	3.5	10

Table 2. T-10 tokamak data for the first and second harmonics.

	B_0 (gauss)	n_e (cm^{-3})	a (cm)	R_0 (cm)	P (MW)	T_e (KeV)	q
1th harmonic	2.78×10^4	0.54×10^{13}	38.7	1.5×10^2	0.75	6.3	9
2nd harmonic	2.47×10^4	0.54×10^{13}	38.7	1.5×10^2	0.45	3.8	9

where $\upsilon = \omega_{pe}^2/\omega^2, u = \Omega^2/\omega^2$ and $\Omega = eB/m_e c$. Here, we have considered the case of an extraordinary wave $(E_1, E_2, 0)$.

Thus, the corresponding components of the ponderomotive force take the form

$$\mathcal{F}_{\alpha 1} = \frac{1}{8\pi}\frac{\upsilon Imk_1}{(1-u)}(1+u)\left|E\right|^2, \tag{26}$$

$$\mathcal{F}_{\alpha 2} = \frac{1}{8\pi}\frac{\upsilon Imk_2}{(1-u)^2}(1+u)\left|E\right|^2. \tag{27}$$

Now, by calculating the average value $\langle \mathbf{B}_0 \cdot \mathcal{F}_\alpha \rangle$ assuming that

$$\begin{aligned} \mathbf{B}_0 &= B_0^\theta \widehat{e}_\theta + B_0^\zeta \widehat{e}_\zeta, \\ \mathcal{F}_\alpha &= \mathcal{F}_{\alpha\psi}\widehat{e}_\psi + F_{\alpha\theta}\widehat{e}_\theta, \end{aligned} \tag{28}$$

and the equation,

$$\mathbf{B}_0 \cdot \mathcal{F}_\alpha = \mathcal{F}_{\alpha\theta} B_0^\theta, \tag{29}$$

and finally substituting (26)-(28) in (29) and averaging, we obtain

$$\langle \mathbf{B}_0 \cdot \mathcal{F}_\alpha \rangle = \frac{B_0 Imk_2}{16\pi^2 q R_0}\left[\frac{\upsilon}{(1-u)^2}\Big((1+u)\left|E\right|^2 + 4\sqrt{u} Im\left(E_1 E_2^*\right)\Big)\right],$$

where it has been considered that

$$\partial_2 \frac{u\upsilon}{(1-u)^2} = \partial_2 \frac{\sqrt{u}\upsilon\,(1+u)}{(1-u)^2} = 0,$$

and the Hamada coordinates [19] have been used.

Finally, neglecting the attenuation of the RF wave, we obtain

$$\langle \mathbf{B}_0 \cdot \mathcal{F}_\alpha \rangle = \frac{B_0 Imk_2}{16\pi^2 q R_0}\frac{\upsilon\,(1+u)}{(1-u)^2}\left|E\right|^2, \tag{30}$$

while the current density related to the ponderomotive force, from (22), assuming the steady state, becomes

$$j_\alpha^{\zeta(p)} \equiv \langle J \rangle \approx \frac{n_\alpha q_\alpha k_2'' |E|^2}{32\pi^3 q R_0^2 m_\alpha n_{\alpha 0}\nu_{\alpha n}}\frac{\upsilon(1+u)}{(1-u)^2}\left(1 + \frac{3}{2}\varepsilon\right). \tag{31}$$

6. Analysis of results.

In order to examine the expression for the current density (31) associated with the ponderomotive force, we adopt the criteria that the deposited energy by the RF wave has to be bigger that the internal enegy ($E^2 > NT$) so to include the nonlinear effects. This condition is satisfied on Tokamaks TCV ad T-10, where an analysis reported in [15, 16] shows that $E^2 \sim 5.75689 \times 10^{13} > NT = 98122.5$ and $E^2 \sim 3.37737 \times 10^{13} > NT = 54500.5$ in these tokamaks, respectively. Such results indicate that the effect of the nonlinear ponderomotive force is highly important in determining the energy density introduced by the RF wave. We will consider a flux cylinder with a radius equal to the Larmor radius so to calculate this energy.

The corresponding data for the TCV and T-10 Tokamaks are summarized in Table 1 and Table 2 [15, 16], respectively. In both reports, the first and second harmonics of the EC waves were used provided that the introduction of the RF wave took place at the high magnetic field (HF) side.

The power associated to the amplitude of the electric field follows from

$$|E|^2 = \frac{2P}{\omega\varepsilon_0}, \tag{32}$$

where P is the power of the wave per time unit and ε_0 is the permittivity in vacuum, assumed to be a constant.

For the imaginary part of the permittivity, $\Im k_2 = k_2^{''}$, we use the expression reported in [17]. In the case of the first harmonic, one has that

$$\frac{k_2^{''}}{k_2} = \frac{2\sqrt{\pi}}{75}\beta_T^2 \left(2-q\right) z^{3/2} e^{-z} \left[\frac{qz^2}{14} + \frac{\left(5/2-q\right)^2}{q\left|F\right|^2}\right], \tag{33}$$

where

$$F\left(z\right) = \frac{3}{4}\left[\frac{1}{2} + z + \sqrt{\pi} z \sqrt{-z} e^{-z}\left(\Phi\left(\sqrt{-z}\right) - 1\right)\right], \tag{34}$$

Here, $\Phi\left(x\right)$ is the error function, $\beta_T = \upsilon_{T_e}/c$ is the ratio of the thermal velocity to the light velocity in vacuum, and $z = 2\left(\Omega - \omega\right)/\Omega\beta_T^2$.

Analogously, for the second harmonic, we have

$$\frac{k_2^{''}}{k_2} = \frac{2^2}{2(5!)}\sqrt{\pi} q \left(1+\Gamma_1\right)^2 z^{3/2} e^{-z}, \tag{35}$$

where

$$\left(1+\Gamma_1\right) = \frac{2^2 - 1 - q\left(1 - 1/2\right)}{2^2 - 1 - q}.$$

The viscosity is neglected while the collision frequency between electrons and neutrals was taken in the form

$$\nu_{en} = \tau_e^{-1} = \left(3.5 \times 10^4 T^{3/2}/n_e\right)^{-1}. \tag{36}$$

It is important to notice that the current density is highly unstable and it depends strongly on the Ω^2/ω^2 relationship. However, it is possible to find an interval where the current density stabilizes and, furthermore, its values reproduce those experimental ones reported in [15, 16], as can be observed in figure 1 and figure 3.

From figure 2 and figure 4, we observe a process in which the Fish and Ohkawa mechanisms weaken each other, as reported in [7]. The general behavior is in good agreement with that described in [8, 18], considering that their calculation was obtained from the linearized Fokker-Planck equation.

Here, the density profile has been modelled as a parabolic one in order to analyze the current, $n_e = n_{0e}\left(1-\frac{2}{3}\left(\frac{r}{a}\right)\right)^2$, where a is the Tokamak minor radius.

It can be noticed in figure 5 that, to first order terms in the parameter ϵ, the driven current density increases with the radius.

7. Conclusions.

The development of a driven current density expression that takes into account the ponderomotive force created by EC waves, has required the use of the neoclassical transport equations up to first order terms with respect to the parameter $\varepsilon = \rho/L$ at a steady state.

The driven current density has been initially obtained in a system of toroidal flux coordinates. That description of the current density is transformed in terms of the Hamada coordinates [19] which is necessary for its validation with experimental results. Thus, the expression for the ponderomotive force reported in [14], is written in a local system of orthogonal coordinates $(\mathbf{e}_1, \mathbf{e}_2, \mathbf{e}_3)$, where $\mathbf{e}_3$ is parallel to the toroidal magnetic field.

The driven current density generated by an extraordinary wave at the cyclotron resonance of electrons, is analyzed as a function of the Ω^2/ω^2 ratio. This is accomplished by using the parameters of the TCV and T-10 Tokamaks at the first and second harmonics, assuming that the introduction of the wave takes place at the HF side. From this results, we have obtained an interval of frequencies, in agreement with the experiments, where the current shows a stable behavior.

In the particular case of a parabolic profile, it has been shown that the ECCD increases with the radius, at first approximation. Finally, it is important to notice that, according to [17], the efficiency is higher for the second harmonic as it is shown in figure 5.

Acknowledgments

This work is partially supported by Conacyt, Mexico, under contract 33873-E.

References

[1] Isayama A *et al* 2000 *Plasma Phys. Control. Fusion* **42** L37
[2] Lin-Liu Y R, Chan V S, *et al* 2003 *Phys. Plasmas* **10** 4064
[3] Prater R 2004 *Phys. Plasmas* **11** 2349

[4] Castejón F *et al* 2004 *Nucl. Fusion* **44** 593
[5] Fish N J and Boozer A H 1980 *Phys. Rev. Lett.* **45** 720
[6] Ohkawa T 1970 *Nucl. Fusion* **15** 185
[7] Cordey J G, Edington T *et al* 1982 *Plasma Phys.* **24** 73
[8] Taguchi M 1989 *Plasma Phys. Contr. Fusion* **31** 241
[9] Alikaev V V *et al* 1995 *Nucl. Fusion* **35** 369
[10] Sauter O *et al* 2001 *Phys. Plasmas* **8** 2199
[11] Matsuda K 1989 *IEEE Trans. Plasma Sci.* **17** 6
[12] Harvey R W and McCoy M G 1993 *Proc. IAEA Technical Comittee Meeting (Montreal, 1992)* p 498
[13] Martinell J J and Gutiérrez-Tapia C 2001 *Phys. Plasmas* **8** 2808
[14] Klima R 1998 *Czech. J. Phys.* **B 18** 1280
[15] Alikaev V V *et al* 1992 *Nucl. Fusion* **32** 1811
[16] Sauter O *et al* 2000 *Phys. Rev. Lett.* **84** 3322
[17] Litvak A G Ed. 1992 *High-frequency Plasma Heating* (New York: AIP press) p 1
[18] Cohen R H 1987 *Phys. Fluids* **30** 2442
[19] Coronado M and Talmadge J N 1993 *Phys. Fluids* **B 5** 1200

Figure captions

Figure 1. Current efficiency plotted against Ω^2/ω^2 for the first harmonic with parametric values from the tokamaks a) T-10 with $f = 140/1.06$ Ghz (solid) and $f = 140/1.12$ Ghz (dashed), and b) TCV with $f = 82.7/1.484$ Ghz (solid) and $f = 82.7/1.5$ Ghz (dashed)

Figure 2. Current efficiency plotted against ε for the first harmonic with values taken by parameters of the tokamaks a) T-10 with $r = 0.0$ cm (solid) and $r = 88$ cm (dashed), and b) TCV with $r = 0.0$ cm (solid) and $r = 88$ cm (dashed).

Figure 3. Current efficiency plotted against Ω^2/ω^2 for the second harmonic with parameters from the tokamaks a) T-10 with $f = 140 \times 0.7$ Ghz (solid) and $f = 140 \times 0.715$ Ghz (dashed) and b) TCV with $f = 82.7 \times 1.331$ Ghz (solid) and $f = 82.7 \times 1.339$ Ghz (dashed).

Figure 4. Current efficiency plotted against ε for the second harmonic with parameter values from the tokamaks a) T-10 with $r = 0.0$ cm (solid) and $r = 88$ cm (dashed), and b) TCV with $r = 0.0$ cm (solid) and $r = 88$ cm (dashed).

Figure 5. Current efficiency plotted against the minor radius r for the second harmonic with parameters from the tokamaks a) T-10 and b) TCV.

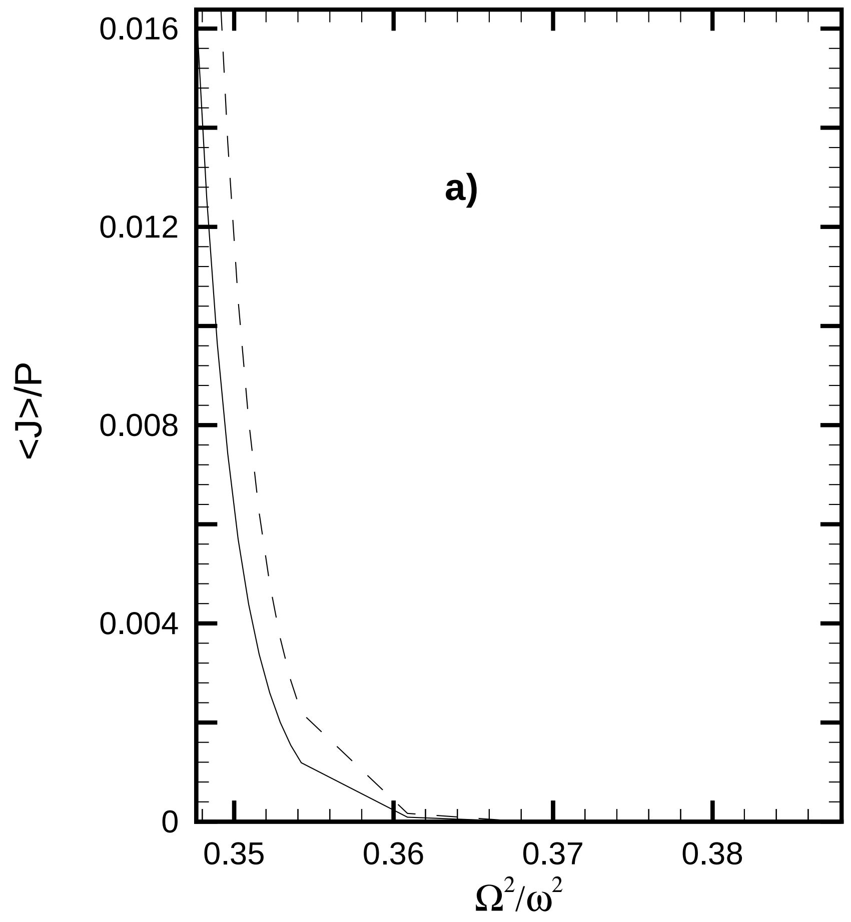
a)
<J>/P
0.016
0.012
0.008
0.004
0
0.35
0.36
0.37
0.38
Ω^2/ω^2

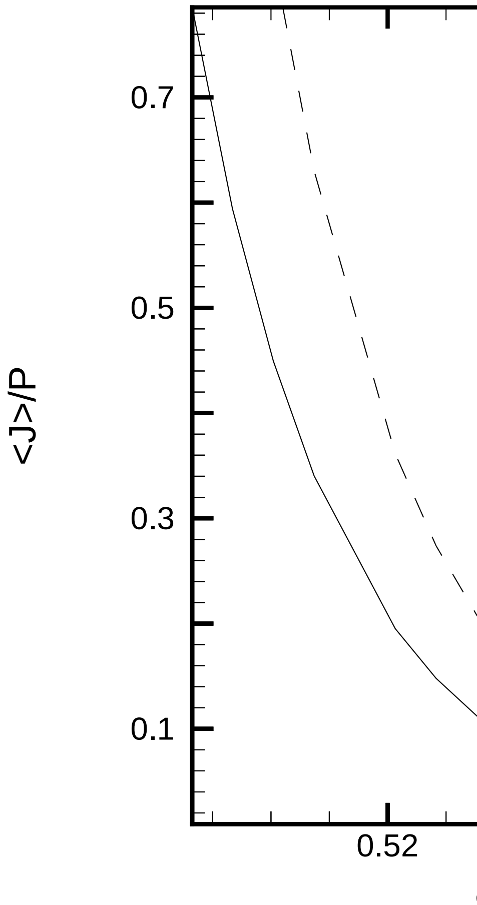
<J>/P
0.7
0.5
0.3
0.1
0.52

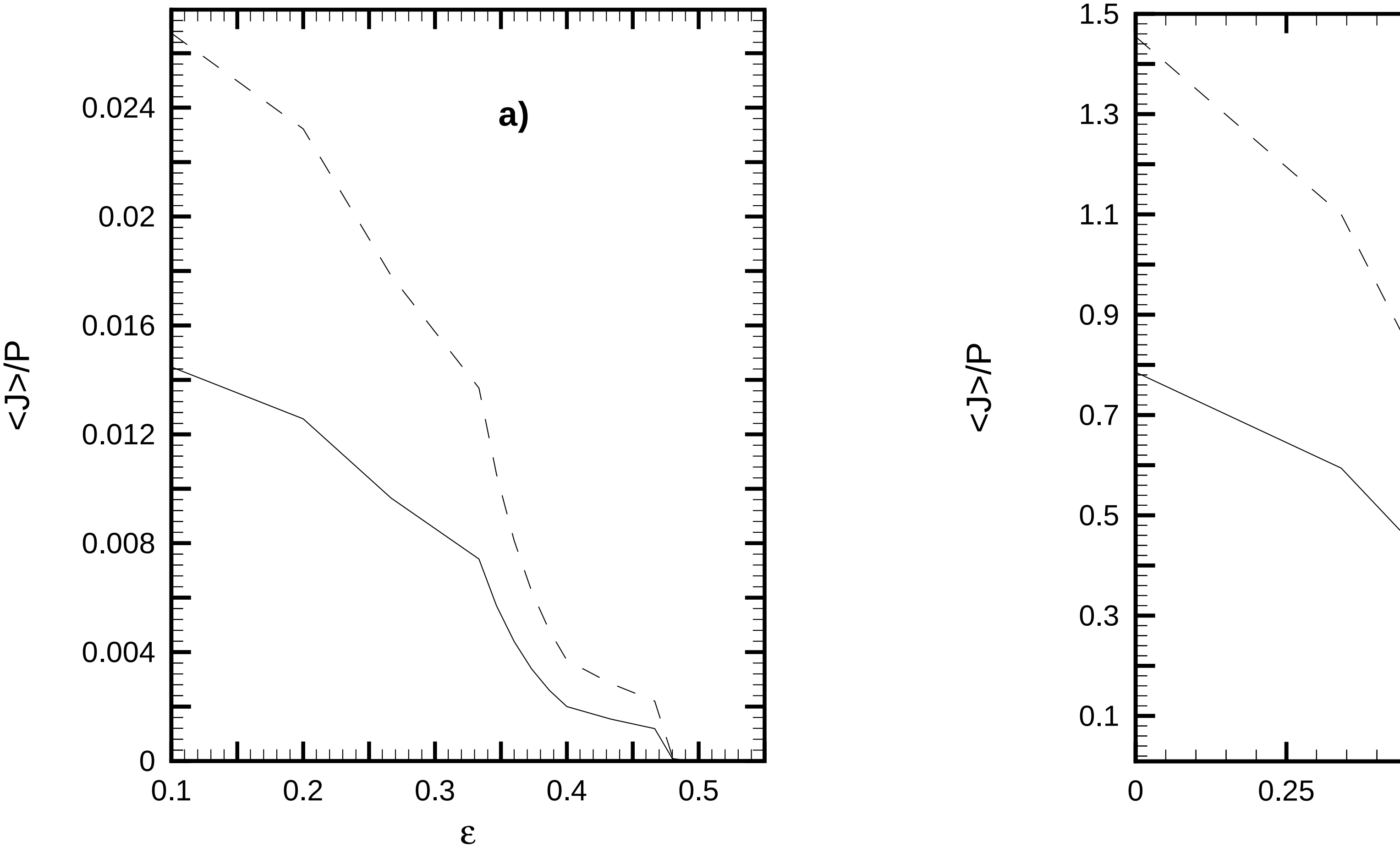
a)
<J>/P
0.024
0.02
0.016
0.012
0.008
0.004
0
0.1
0.2
0.3
0.4
0.5
ε
<J>/P
1.5
1.3
1.1
0.9
0.7
0.5
0.3
0.1
0
0.25

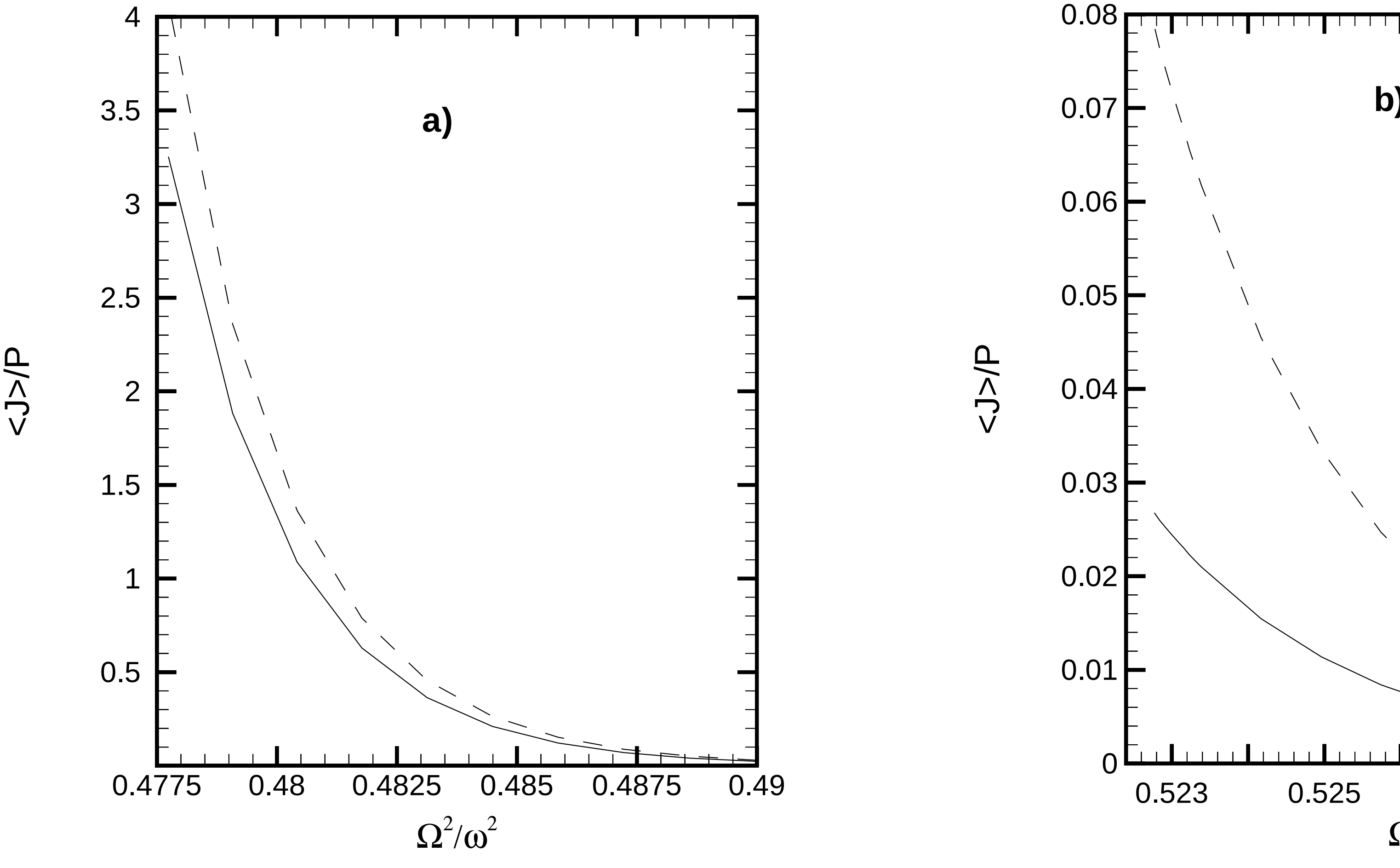
a)
<J>/P
4
3.5
3
2.5
2
1.5
1
0.5
0.4775
0.48
0.4825
0.485
0.4875
0.49
Ω^2/ω^2
b
<J>/P
0.08
0.07
0.06
0.05
0.04
0.03
0.02
0.01
0
0.523
0.525
Ω

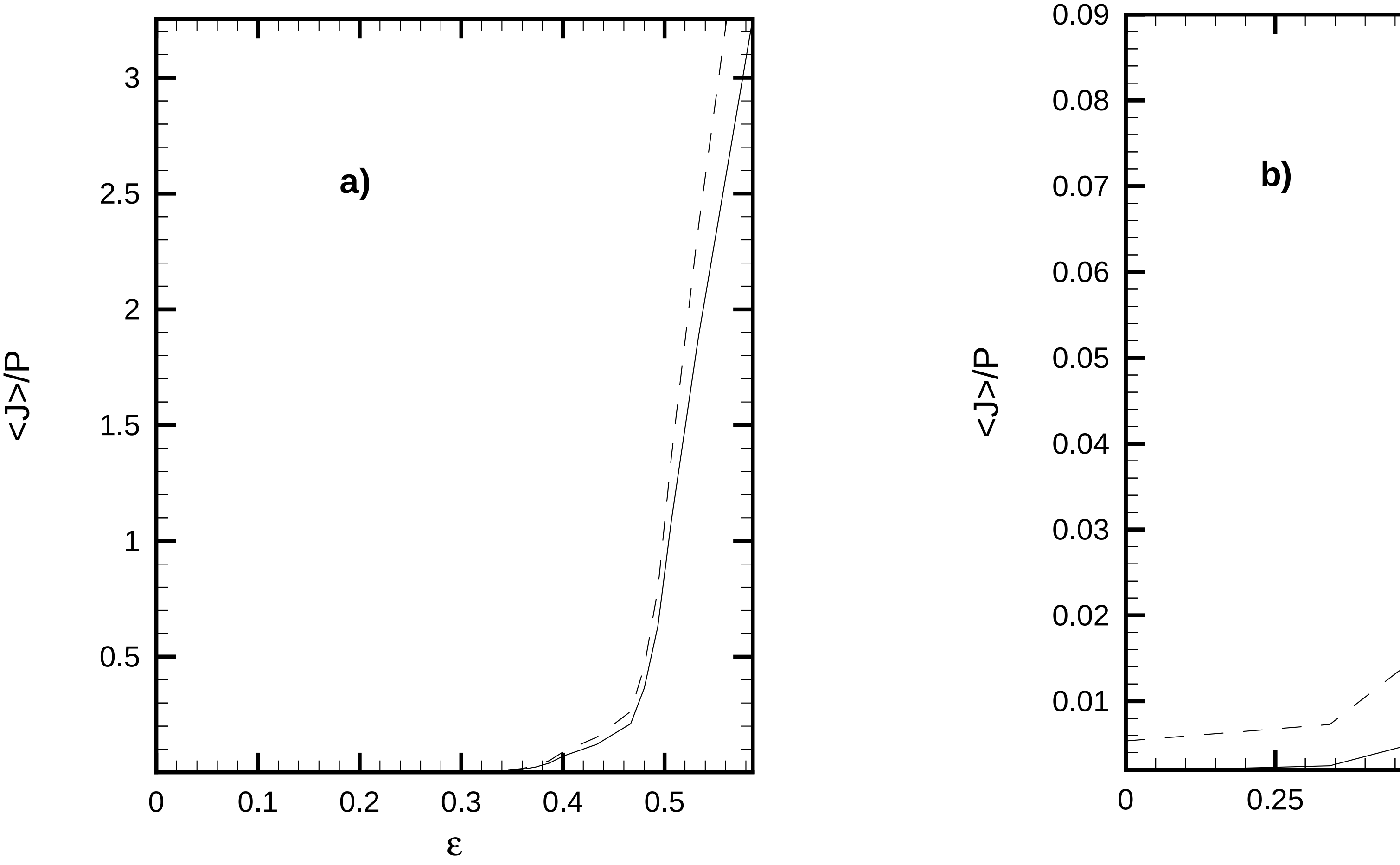
a)
<J>/P
0.5
1
1.5
2
2.5
3
0
0.1
0.2
0.3
0.4
0.5
ε
b)
<J>/P
0.01
0.02
0.03
0.04
0.05
0.06
0.07
0.08
0.09
0
0.25

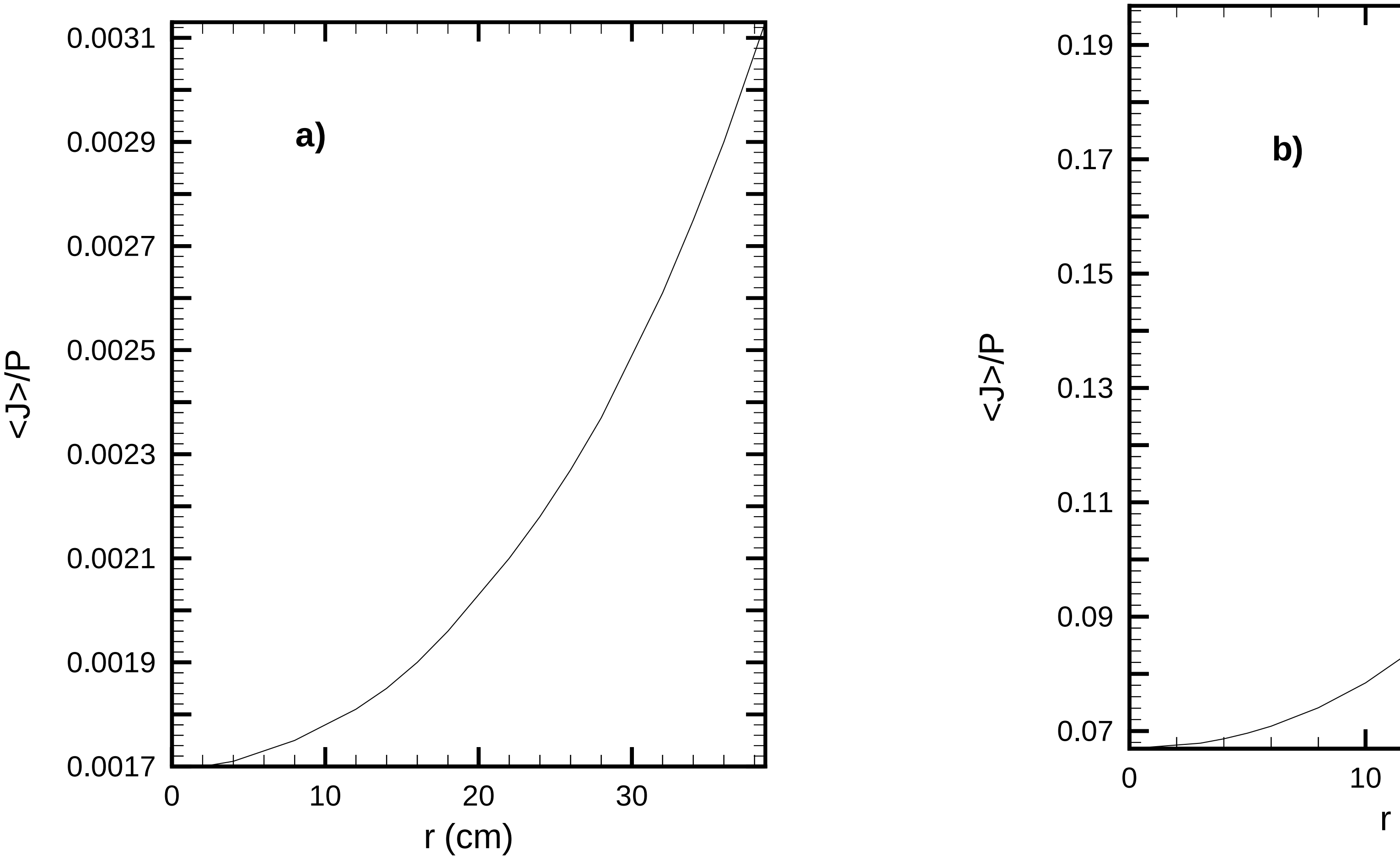
a)
<J>/P
0.0031
0.0029
0.0027
0.0025
0.0023
0.0021
0.0019
0.0017
0
10
20
30
r (cm)
b)
<J>/P
0.19
0.17
0.15
0.13
0.11
0.09
0.07
0
10
r